Estrogen receptor β regulates AKT activity through up-regulation of INPP4B and inhibits migration of prostate cancer cell line PC-3

Surendra Chaurasiya[a], Wanfu Wu[a], Anders M. Strom[a], Margaret Warner[a], and Jan-Åke Gustafsson[a,b,1]

[a]Department of Biology and Biochemistry, Center for Nuclear, Receptors and Cell Signaling, Science & Engineering Research, University of Houston, Houston, TX 77204-5056; and [b]Department of BioSciences and Nutrition, Karolinska Institute, SE-14157 Huddinge, Sweden

Contributed by Jan-Åke Gustafsson, September 8, 2020 (sent for review April 14, 2020; reviewed by Sari Makela and Ganesh Palapattu)

Loss of the tumor suppressor, PTEN, is one of the most common findings in prostate cancer (PCa). This loss leads to overactive Akt signaling, which is correlated with increased metastasis and androgen independence. However, another tumor suppressor, inositol-polyphosphate 4-phosphatase type II (INPP4B), can partially compensate for the loss of PTEN. INPP4B is up-regulated by androgens, and this suggests that androgen-deprivation therapy (ADT) would lead to hyperactivity of AKT. However, in the present study, we found that in PCa, samples from men treated with ADT, ERβ, and INPP4B expression were maintained in some samples. To investigate the role of ERβ1 in regulation of INPPB, we engineered the highly metastatic PCa cell line, PC3, to express ERβ1. In these cells, INPP4B was induced by ERβ ligands, and this induction was accompanied by inhibition of Akt activity and reduction in cell migration. These findings reveal that, in the absence of androgens, ERβ1 induces INPP4B to dampen AKT signaling. Since the endogenous ERβ ligand, 3β-Adiol, is lost upon long-term ADT, to obtain the beneficial effects of ERβ1 on AKT signaling, an ERβ agonist should be added along with ADT.

prostate cancer | estrogen receptor | INPP4B | androgen deprivation therapy

Prostate cancer (PCa) is the most common cancer in US men and second leading cause of cancer-related death (1). While primary PCa is indolent in nature, metastatic cancer is a fatal disease (2).

Hyperactive PI3K/AKT signaling pathway has been implicated in growth and survival, and epithelial-mesenchymal transition (EMT), angiogenesis, metastasis, and development of chemoresistance are seen in a wide range of tumors (3). Upon activation by growth factors and other mitogenic signals, the enzyme, PI3K, generates the lipid second messenger PI(3,4,5)P3, which is the biological activator of AKT. Fully activated AKT can then phosphorylate many downstream proteins, resulting in enhanced survival, proliferation, metabolism, and migration (4).

The phosphatase, PTEN, is the major negative regulator of this pathway. It removes the 3′ phosphate of PI(3,4,5)P3 to produce PI(4,5)P2, which cannot activate AKT. In the absence of functional PTEN, there is accumulation of PI(3,4,5)P3, leading to increased AKT activity (5). In PCa, complete loss of PTEN is associated with increased metastasis and androgen independence (6, 7). Loss of PTEN occurs at high frequency in PCa where up to 60% is monoallelic loss in primary cancer and 100% in metastatic cancer (8). Another phosphatase, inositol-polyphosphate 4-phosphatase type II (INPP4B), removes the 4′ phosphate in PI(3,4)P2 and can partially compensate for the loss of PTEN (9, 10). Concomitant loss of PTEN and INPP4B expression leads to accumulation of PI(3,4,)P2 increasing AKT activity (11). Similar to the loss of PTEN, loss of INPP4B is also associated with increased aggressiveness and metastasis of PCa (12).

The estrogen receptor β (ERβ1) functions as a tumor suppressor in various cancers (13–15). In addition, genomic deletion of ERβ in mouse leads to prostatic epithelial hyperplasia and up-regulation of AR-regulated genes in the prostate (16). Multiple tumor suppressive mechanisms of ERβ1 have been described. It inhibits cell proliferation by up-regulating p21, p27, and/or down-regulating p45 SKp2 (17). It induces apoptosis in PCa cell lines through up-regulation of PUMA and FOXO3a (18), impedes EMT in triple negative breast cancer (TNBC) cells by suppressing EGFR signaling (19), and decreases the invasiveness of TNBC cells by inhibiting mutant p53 function (20).

Multiple studies have described antiproliferative and proapoptotic effects of ERβ1 in various cancers; however, the role of ERβ1 in metastasis needs further investigation. Expression of ERβ usually declines as tumors progress above Gleason grade 3 + 3 in PCa (21, 22). However, there are reports of reexpression of ERβ in some advanced PCa as well as in metastatic tumors (23, 24). While in breast cancer ERβ1 inhibits metastasis through regulating EMT (19, 20), the role of ERβ1 in PCa metastasis remains to be determined.

Dysregulation of PI3K/AKT/PTEN signaling is one of the most common characteristics of PCa (6, 7). ERβ1 up-regulates PTEN in breast cancer cell lines (25) and, in the mouse prostate, ERβ agonists drive PTEN into the nucleus where it has a strong antiproliferative role (16). In the present study, we used immunohistochemistry to analyze the expression of ERβ1 and INPP4B in advanced PCa tissues. Additionally, using stable ERβ1 expressing PC3, BPH, and LNCaP cells, we investigated the regulation of PI3K/AKT activity by ERβ1. We also used the wound healing assay to investigate the

Significance

Dysregulation of PI3K/AKT/PTEN signaling is a common characteristic of prostate cancer (PCa). Loss of the tumor suppressor PTEN occurs frequently in PCa and leads to overactive AKT signaling. Complete loss of PTEN is associated with increased metastasis and castration resistance in PCa. However, another tumor suppressor, inositol-polyphosphate 4-phosphatase type II (INPP4B), can partially compensate for the loss of PTEN. INPP4B is up-regulated by the androgen receptor, and androgen deprivation therapy (ADT) would be expected to lead to hyperactive AKT due to concomitant loss of both PTEN and INPP4B. However, the present study shows that ERβ agonists induce expression of INPP4B and down-regulate AKT. This study provides a rationale for further investigations to understand the role of ERβ1 in advanced PCa.

Author contributions: S.C. and J.-Å.G. designed research; S.C., W.W., and A.M.S. performed research; S.C., W.W., A.M.S., M.W., and J.-Å.G. analyzed data; and S.C., A.M.S., M.W., and J.-Å.G. wrote the paper.

Reviewers: S.M., University of Turku; and G.P., University of Michigan Medical School.

The authors declare no competing interest.

[1]To whom correspondence may be addressed. Email: jgustafsson@uh.edu.

This article contains supporting information online at https://www.pnas.org/lookup/suppl/doi:10.1073/pnas.2007160117/-/DCSupplemental.

First published October 5, 2020.

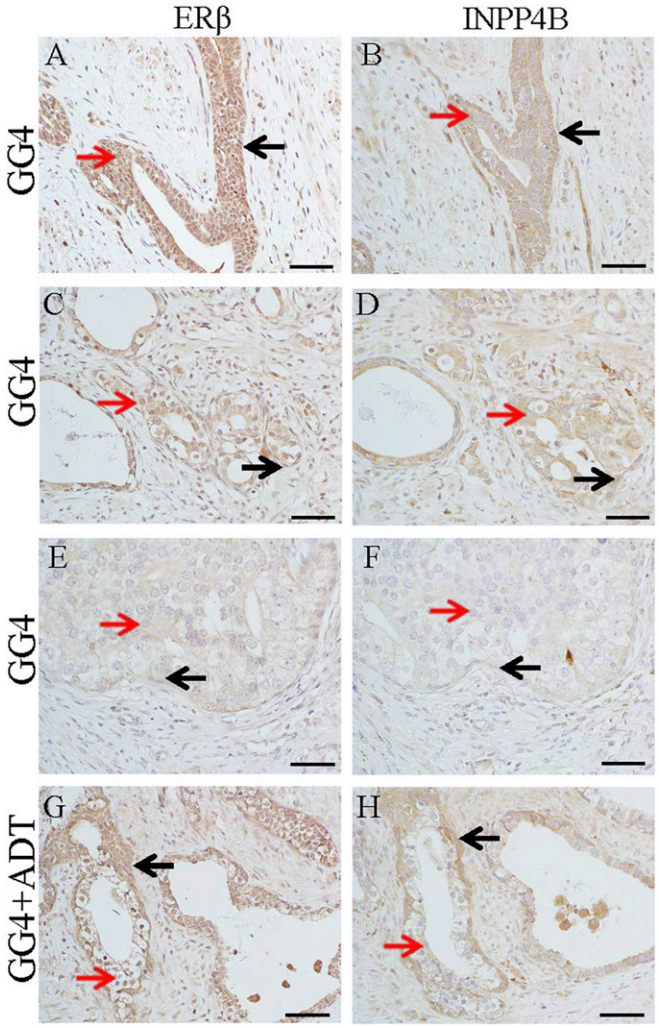

Fig. 1. Expression pattern of ERβ and INPP4B in GG4 PCa. In normal parts of PCa tissues, ERβ was expressed in nuclei of luminal (red arrow) and myoepithelial (black arrow) cells (*A*). INPP4B was expressed in luminal (red arrow) and myoepithelial (black arrow) cells (*B*). In PCa with fused glands where ERβ was still expressed in epithelial cells (*C*) INPP4B was also present in epithelial cells (*D*). In PCa where ERβ was undetectable in epithelial cells (*E*) INPP4B expression was extremely low (*F*). In ADT-treated PCa there was desquamation of epithelial cells (red arrow) as expected. ERβ-positive myoepithelial cells (*G*) were intact and INPP4B was still detectable in these cells (black arrow) (*H*). (Scale bars in *A*–*H*, 50 μm.) (GG4, Gleason grade 4; ADT, Androgen deprivation therapy.)

ability of ERβ1 to inhibit migration of PC3 cells in vitro. In the present study, we show that in ADT-treated men, ERβ and INPP4B expression are maintained in the prostate; that ERβ1 inhibited PC3 cell migration by inhibiting AKT activity through INPP4B up-regulation; and using chromatin immunoprecipitation (ChIP)-sequencing (seq) assays, we found that ERβ1 binds to two enhancers in INPP4B gene. Thus, one benefit of ADT is increased expression of ERβ1.

Results

ERβ and INPP4B Expression in PCa Tissues. A relationship between ERβ, INPP4B, and AR was noted in a cohort of men with Gleason grade 4 cancers who were receiving ADT (Fig. 1). Biopsies from these prostates showed that, although they were expected to express very little ERβ, of 436 samples stained 180 (41%) were positive for ERβ. Some samples expressed strong nuclear ERβ in both the luminal epithelium and myoepithelium. As expected, ADT treatment led to desquamation of luminal epithelial cells, but myoepithelial cells remained and were positive for both ERβ and INPP4B. INPP4B was expressed in the cytoplasm of the ERβ-positive cells. In the normal ducts present in the PCa samples, both ERβ and INPP4B were still expressed in epithelial cells.

These data suggested the hypothesis that ADT increased expression of ERβ and that INPP4B is an ERβ-regulated gene. This hypothesis was addressed in cell lines as shown below.

Stable Expression of ERβ1 in PCa Cell Line PC3 and BPH1. Expression of ERβ is gradually reduced during progression of PCa, and cell lines established from metastatic disease express very low levels of ERβ1 (26). In the present study, we used PCa cell line PC3 and benign prostate epithelial cell line BPH1 to study the effect of ERβ1. The PC3 cell line was established from bone metastasis of a stage IV (advanced) PCa patient. These cells are highly metastatic in xenograft animal models and exhibit high motility in cell culture (27). They do not express androgen receptor and express very low levels of ERβ1. It is thought that PC3 cells represent poorly differentiated adenocarcinoma (28). BPH1 cells are immortalized benign prostate cell line of basal type. These cells express Δp63 as well as cytokeratin 5 and 14 (29).

We expressed ERβ1 in PC3 and BPH1 cells using lentivirus-mediated gene delivery and integration and selected for at least 2 wk before using the cells in experiments. Stable expression of ERβ1 was detected using RT-qPCR, Western blotting, and immunofluorescence in PC3 cells (*SI Appendix*, Fig. S1).

ERβ1 Up-Regulates INPP4B in PC3 and BPH1 Cells. RNA-seq analysis was used to compare the gene expression profiles of PC3 cells expressing ERβ1 with control PC3 cells. Cells were treated with either vehicle (DMSO) or ERβ-selective ligand LY3201. One of the genes whose expression was increased >3.5-fold in ERβ1-expressing cells treated with LY3201 was INPP4B (Table 1). We validated INPP4B up-regulation with qPCR and Western blotting and confirmed the ERβ regulation with additional ERβ ligands, DPN and estradiol (E2). Cells infected with empty vector, which expresses antibiotic resistance gene but no ERβ1, were used as controls in all experiments. While INPP4B in control cells was only detectable upon longer exposure of Western blot membranes, it was readily detected in PC3 cells expressing ERβ1. The expression of INPP4B was ligand-dependent with the highest induction in cells treated with LY3201. ERβ1 also up-regulated INPP4B in BPH1 cells both at transcript and protein level (Fig. 2).

ERβ1 Inhibits AKT Activity in PC3 Cells. Since INPP4B catalyzes the dephosphorylation of PI(3,4)P2-producing PI(3)P (30), which cannot activate AKT activity (9), we investigated whether ERβ1 inhibition of AKT activity was mediated by induction of INPP4B. We found that ERβ1-mediated induction of INPP4B was accompanied by significant reduction of AKT phosphorylation on Ser473 in PC3 cells (Fig. 3), while AKT phosphorylation on Thr308 was not detectable in either control or ERβ1-expressing cells. In confirmation of the inhibition of AKT activity, the phosphorylation of GSK3β, a substrate of AKT (31), decreased along with pAKT Ser473 in ERβ1-expressing cells.

Table 1. RNA-seq result showing differential regulation of INPP4B by ERβ1 in PC3 cells

Symbol	Treatment	$\log_2$ FC	*P* value
INPP4B	DMSO	0.19	0.77 (NS)
INPP4B	LY3201	1.87	0.005

NS: not significant.

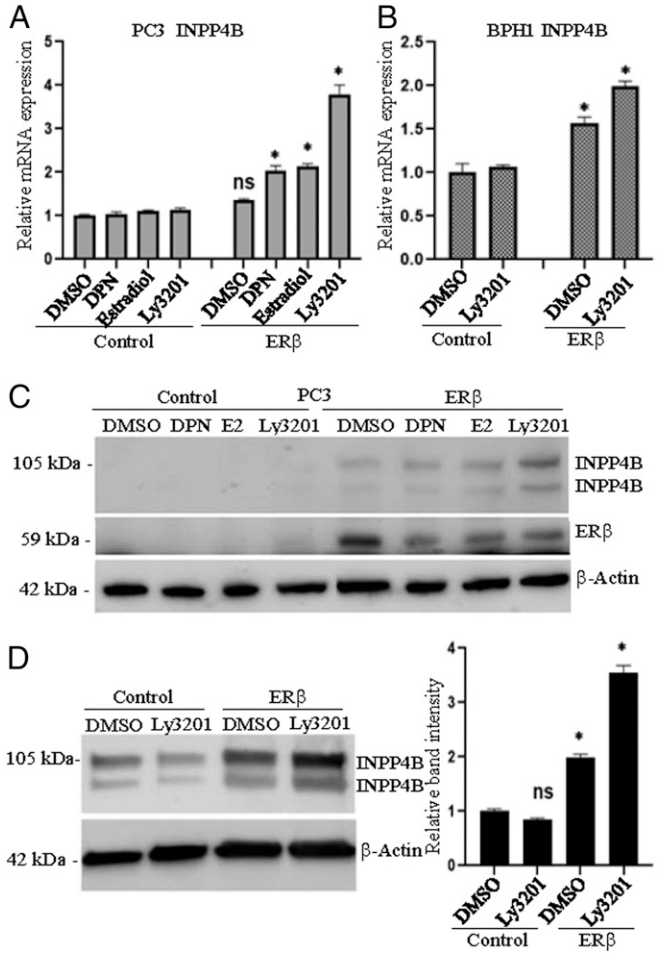

Fig. 2. ERβ1 induces expression of INPP4B in PC3 and BPH1 cells. Stable PC3 and BPH1 cells were grown to 60% confluency and treated with ligands in 10% DCC-FBS for 24 h; RNA and protein were extracted and analyzed for expression of INPP4B. (*A*) Expression of INPP4B mRNA in PC3 control and ERβ1 cells. (*B*) Expression of INPP4B mRNA in BPH1 control and ERβ1 cells. Values presented as fold difference compared with control DMSO and represent mean ± SEM of three independent experiments (*$P < 0.05$). (*C*) Expression of INPP4B protein in PC3 control and ERβ1 cells. (*D*) Western blot of INPP4B protein in BPH1 control and ERβ1 cells, quantification of band intensity (*Right*). ns, not significant.

ERβ1 Repression of AKT Activity Is Dependent on INPP4B Up-Regulation. To confirm that inhibition of AKT activity by ERβ1 is mediated through INPP4B, we reduced INPP4B expression in ERβ1-expressing PC3 cells with small-interfering RNA (siRNA). Western blotting of cell lysates revealed that the level of pAKT (Ser473) increased while total AKT did not change (Fig. 4).

ERβ1 Inhibits Migration of PC3 Cells. Wound healing assays are commonly used to measure collective cell movement on a two-dimensional substrate (32). A wound is made on a confluent sheet of monolayer cells, and image of the wound is captured and incubated in desired condition for a certain period to allow migration of cells into the empty area. At the end, image is taken again, and the gap in the wound is compared with control (33).

We used this assay to measure the effect of ERβ1 expression on PC3 cell migration. Cells were treated with LY3201 for 18 h in phenol red-free RPMI supplemented with 10% dextran coated charcoal (DCC)-fetal bovine serum (FBS). Images of the wound were taken before and after incubation and analyzed with ImageJ software. We found that ERβ1-expressing cells migrated more slowly than control cells (Fig. 5).

Depletion of INPP4B Abrogates Effect of ERβ1 on Cell Migration. The PI3K/AKT pathway activity is implicated in cell survival, proliferation, and migration. Hyperactive AKT activity is strongly associated with EMT and tumor metastasis (34). We investigated whether inhibition of PC3 cell-migration in ERβ1-expressing cells is regulated through INPP4B. When INPPB4 siRNA was

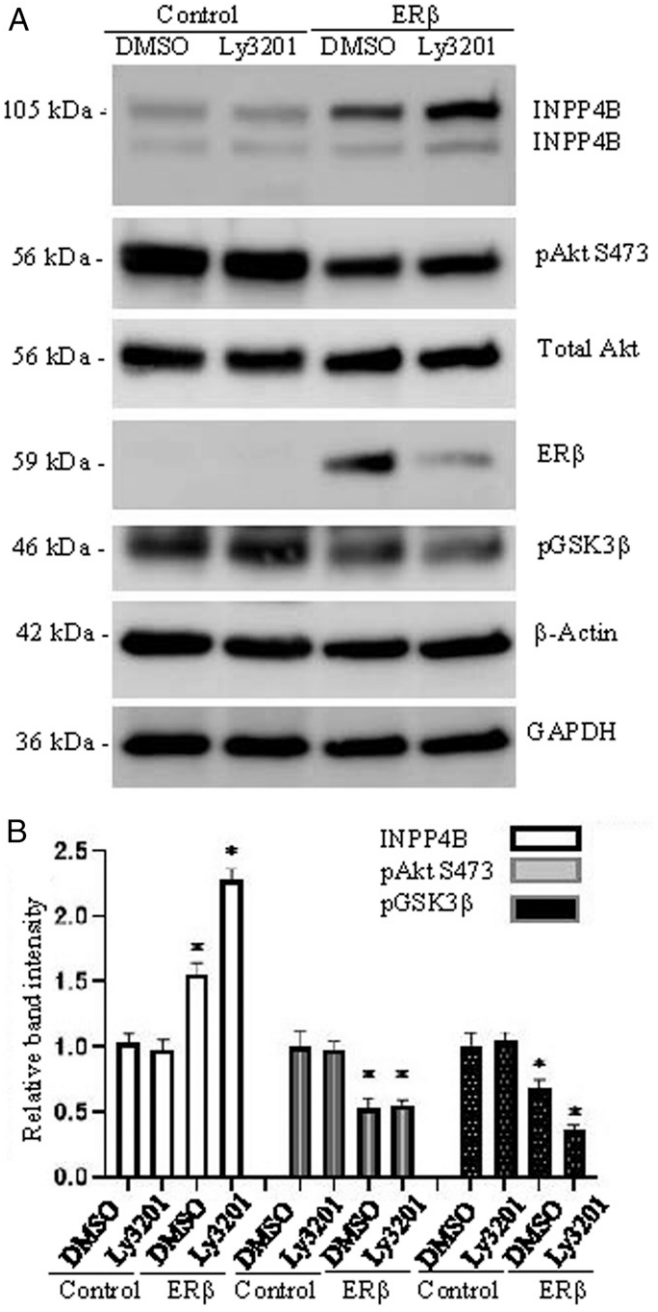

Fig. 3. ERβ1 inhibits AKT activity in PC3 cells. Stable PC3 cells were grown to 60–70% confluency, treated in 10% DCC-FBS for 24 h with DMSO or LY3201, and analyzed for indicated proteins. (*A*) Representative Western blot for INPP4B, pAKT S473, Total AKT, ERβ1, pGSK3β, β-Actin, and GAPDH. (*B*) Band intensity for INPP4B, pAKTS473, and pGSK3β. GAPDH was used as normalizing control. Values are presented as fold difference compared with control DMSO and represent mean ± SEM of three independent experiments (*$P < 0.05$).

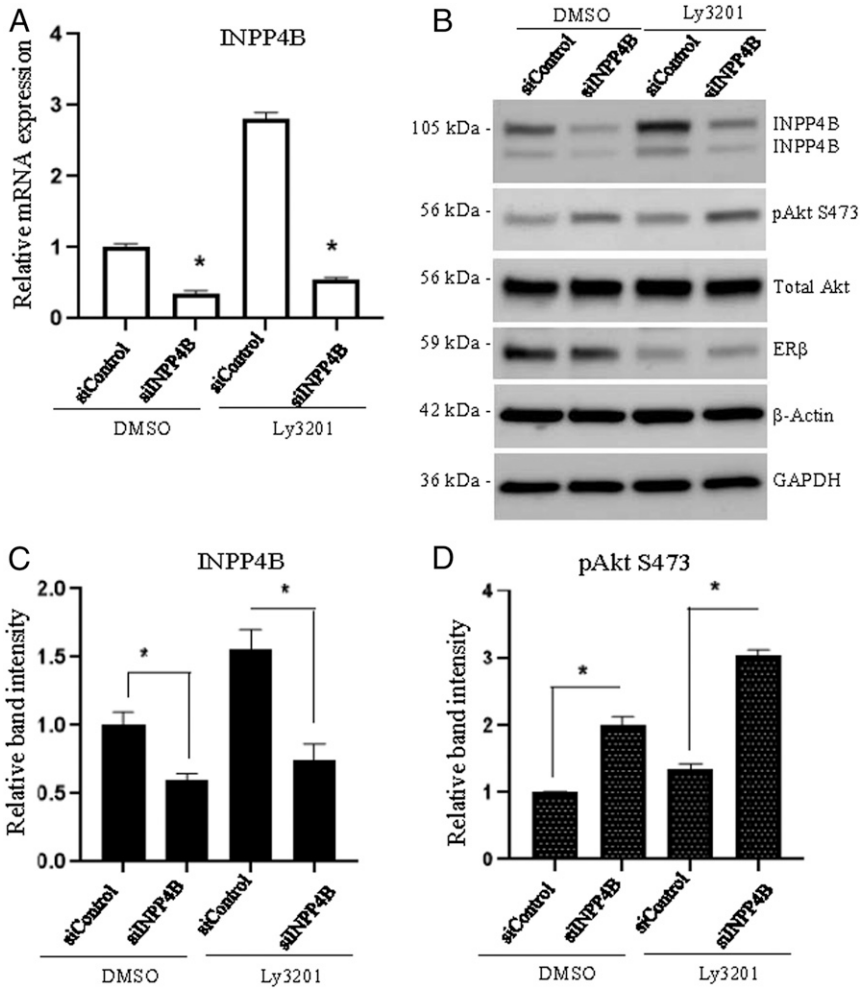

Fig. 4. Knockdown of INPP4B increases AKT activity in PC3 ERβ1 cells. PC3 ERβ1 cells were transfected with INPP4B or negative control siRNA for 48 h and treated with DMSO or LY3201 in 10% DCC-FBS for 24 h. (*A*) Relative mRNA expression of INPP4B in siControl and siINPP4B PC3 ERβ1 cells. (*B*) Protein expression of INPP4B, pAKT S473, Total AKT, ERβ1, β-Actin, and GAPDH in siControl and siINPP4B PC3-ERβ1 cells. (*C* and *D*) Band intensities of INPP4B and pAKT S473 of siControl and siINPP4B PC3 ERβ1 cells. Values are presented as fold difference compared with control DMSO and represent mean ± SEM of three independent experiments (*$P < 0.05$).

expressed in the ERβ1-expressing PC3 cells, there was faster migration in wound healing assay (Fig. 6). The effect was modest but statistically significant, indicating that there may be additional factors influencing migration in these cells or that the INPPB4 siRNA did not completely eliminate INPP4B from the cells.

INPP4B Is a Direct Target Gene of ERβ1. Global ChIP-seq was used to elucidate the mechanism of INPP4B up-regulation by ERβ1. We found that ERβ1 bound to two intronic sequences in the INPP4B gene, which we named enhancer 1 and enhancer 2 relative to the promoter of the gene (Fig. 7). We also analyzed a 400-bp stretch of DNA from the enhancers using Position Specific Scoring Matrices (Possum) (35) for the enriched cis-elements. Possum analysis resulted in common and uncommon motifs being enriched in these enhancers (Fig. 8). For enhancer 1, whose peak is smaller and closer to the promoter, two EREs, two AP1, and two GATA motifs were found. Of the two EREs, one is perfect and the other imperfect ERE. The largest score was for the perfect ERE followed by AP1 and CCAAT. Some uncommon motifs CCAAT, SRF, LSF, Ets, NF-1, and TATA were also enriched. The CCAAT motif is located adjacent to the perfect ERE, which raises the possibility of interaction between ERβ1 and C/EBPs (CCAAT enhancer binding proteins). For enhancer 2, which appeared to have a larger peak, the cis-elements found were 1/2 EREs, Sp1, Tef, Mef-2, LSF, CRE, and CCAAT. Interestingly, no AP1 elements were enriched. Again, the largest score was for 1/2 ERE followed by Sp1 and LSF.

ERβ1 Regulates Transcription from the INPP4B Enhancers. Next, we evaluated the ability of ERβ1 to induce transcription from these two regions (enhancer 1 and enhancer 2) using luciferase reporter assay. A 500-bp stretch of DNA was PCR amplified from genomic DNA containing enhancers and cloned into a pGL3-promoter luciferase reporter. PC3 cells were transfected with one of these constructs with or without ERβ1 expression vector and treated with LY3201 for 24 h in 10% DCC-FBS. We found that ERβ1 induced a robust ligand-dependent expression of luciferase from these enhancers. In this assay, enhancer 1 showed higher induction than the enhancer 2 (Fig. 9).

Discussion

Discovery of ERβ expanded the domain of estrogen signaling. While ERα has been implicated in various endocrine-dependent cancers (36), ERβ1 emerged as a tumor suppressor. ERβ1 exerts tumor suppressor activity through various mechanisms including

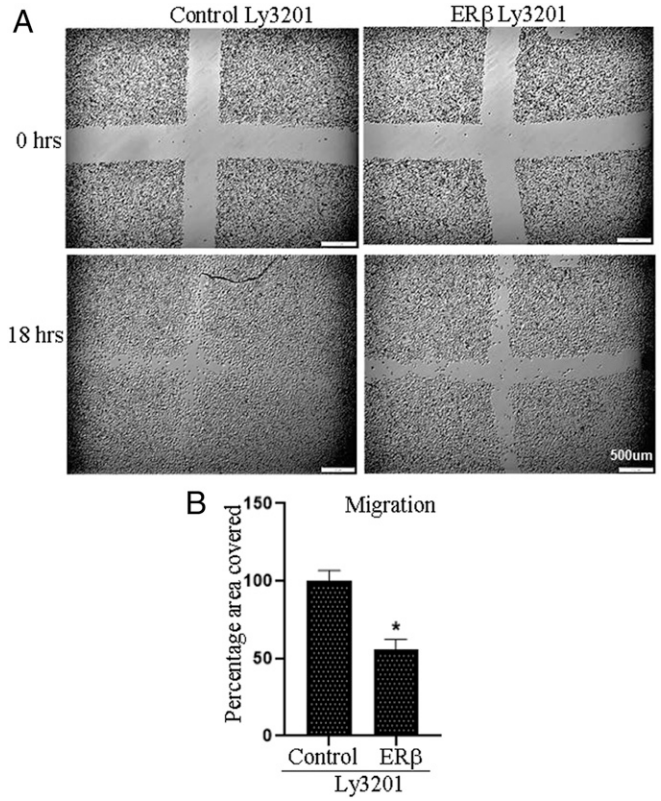

Fig. 5. ERβ1 inhibits migration of PC3 cells. (*A*) PC3 control and ERβ1 stable cells were grown to confluency in a six-well plate, and a wound was made with a pipette tip. Cells were incubated with LY3201 for 18 h in 10% DCC-FBS. Images were taken initially (0 h) and after the end of incubation (18 h). (*B*) Quantification of cell migration; empty spaces in all images were delineated and measured with ImageJ software. Total area covered in control cells at the end of incubation (18 h) was set as 100%. Initial empty area from (0 h) was used for normalization. $*P < 0.05$.

inhibition of proliferation (13–15), induction of apoptosis (18), and inhibition of epithelial to mesenchymal transition (19).

INPP4B is a phosphatase belonging to PI3K/AKT pathway where it negatively regulates PI3K signaling by removing the four-phosphate group from PI(3,4)P2 (9, 30). In normal cells, PTEN is the major regulator of PI3K/AKT, but PTEN is frequently lost in PCa, leading to overactivated AKT (6, 8). The question we addressed in the present study is whether ERβ1 can regulate AKT activity and substitute for the loss of PTEN in PCa.

We first examined expression of INPP4B in human PCa of different Gleason grades and found high expression of INPP4B in some samples. Surprisingly, however, in men treated with ADT, INPP4B expression was maintained, suggesting that this enzyme was regulated by pathways that did not involve androgens.

As we began to investigate alternative regulation of INPP4B, we noted that in an RNA-seq study of glioblastoma cells stably expressing ERβ1, treatment with Ly5003007 (an ERβ selective agonist) induced expression of INPP4B (14). Several reports have described an inhibitory effect of INPP4B expression on cell migration. Exogeneous expression of INPP4B in PC3 and DU145 cells significantly inhibited migration and/or invasion in transwell assays, and this was found to be mediated through inhibition of AKT activity (37, 38). We, therefore, engineered PC3 cells to express ERβ1 and found that INPP4B was induced >3.5-fold.

PC3 cells express neither PTEN nor AR (27). The up-regulation by ERβ1 of a gene, which is AR-up-regulated, is unexpected because ERβ1 opposes AR transcriptional activity (16). We tested whether expression of ERβ1 in PC3 cells affected AKT activity. AKT activity is regulated by phosphorylation at Thr308 and Ser473 (39). In PC3 cells, pAKT Thr308 could not be detected but pAKT Ser473 level was decreased by ∼50%. We hypothesized that decrease in AKT activity is due to increase in INPP4B.

To test this hypothesis, we partially decreased INPP4B level in PC3-ERβ1 cells using siRNA and observed that pAKT Ser473 level increased. This finding lead to the conclusion that ERβ1 regulates AKT activity through up-regulation of INPP4B.

AKT activity has been implicated in many biological processes such as survival, proliferation, and migration of cells. Overactive AKT activity is widely associated with aggressiveness of tumors and enhanced metastasis (6, 7). To understand the biological effect of AKT inhibition, we used the wound healing assay with stable PC3-ERβ1 cells. We observed that PC3-ERβ1 cells migrated significantly slower than control cells. To confirm that this effect is mediated through INPP4B, we used the wound healing assay on PC3-ERβ1 cells after knock-down of INPP4B with siRNA. As expected, siINPP4B-transfected cells migrated faster than control siRNA-transfected cells.

To understand the mechanism of INPP4B up-regulation by ERβ1, we analyzed global ERβ1-binding regions in PC3 cells. ChIP-seq revealed two locations in INPP4B genes where ERβ1 was bound. We further analyzed DNA sequences in a 400-bp stretch of those two ERβ1-binding enhancers in INPP4B. Possum

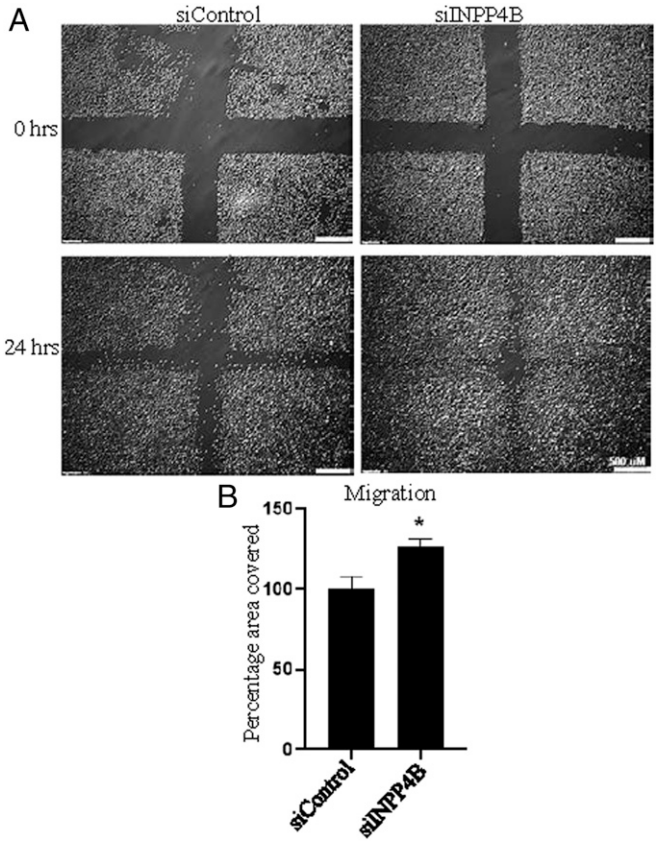

Fig. 6. ERβ1 inhibited migration is dependent on level of INPP4B. (*A*) PC3 ERβ1 stable cells were grown to 50–60% confluency in 6-well plate and transfected with negative control (siControl) or INPP4B siRNA. After 48 h a wound was made with a pipette tip. Cells were incubated with LY3201 for 24 h in 10% DCC-FBS. Images were taken initially (0 h) and after the end of incubation (18 h). (*B*) Quantification of cell migration; empty spaces in all images were delineated and measured with ImageJ software. Total area covered in siControl cells at the end of incubation (18 h) was set as 100%. Empty area from initial (0 h) was used for normalization.

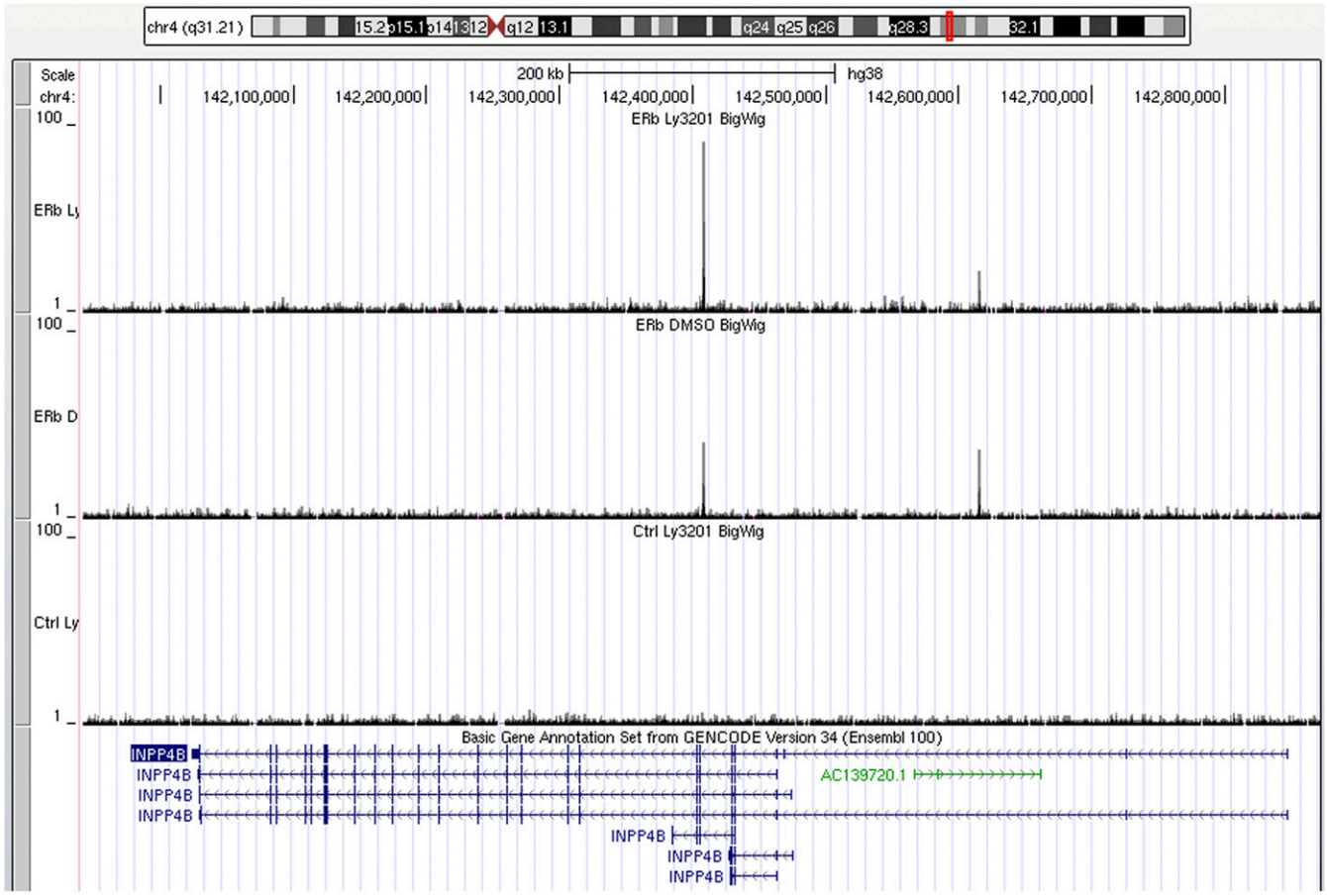

Fig. 7. ERβ1 binds to intron of INPP4B gene. A screen shot of ERβ1 binding to UCSC genome browser extending INPP4B gene.

analysis revealed >15 cis-elements including ERE, 1/2 ERE, AP1, and SP1 among others being enriched in a small region. These motifs may indicate possible cooperation of different transcription factors involved in INPP4B regulation by ERβ1. Androgen receptor was shown to bind near INPP4B gene (40), but both ERβ1 binding loci are different from AR-binding region.

INPP4B functions as a tumor suppressor in PCa and is lost in advanced stages of the disease. It is regulated by the androgen receptor in LNCaP cells where it inhibits AKT activity (40). Thus, it could be anticipated that androgen ablation therapy would increase AKT activity because of the loss of INPP4B expression. Our findings suggest that treatment with ERβ-specific agonists can benefit patients with PTEN loss and overactive AKT signaling. One further benefit of AKT inhibition is an increase in apoptosis (41). Our data, therefore, adds to the mechanisms through which ERβ1 induces apoptosis in PCa (18) by targeting the AKT/FOXO3a/PUMA survival pathway.

Materials and Methods

Reagents and Cell Culture. PC3 and BPH1 cell lines were obtained from the American Type Culture Collection and were propagated in RPMI 1640 (Invitrogen Inc.) medium supplemented with 10% FBS (Sigma), and Anti-Anti (Invitrogen Inc.) at 37 °C and 5% CO_2. All ligand-treatment experiments were performed in phenol red-free medium supplemented with 10% dextran coated charcoal (DCC)-treated FBS. Ly3201 was provided by Eli Lily Company. 17β-estradiol, DPN, and Bicalutamide was purchased from Millipore Sigma.

Stable Expression of ERβ1 in PC3 and BPH1 Cells. Early passage of PC3 and BPH1 cells were infected with the lentivirus Lenti6-TOPO-V5-D empty or containing complementary DNA (cDNA) for human ERβ1 at 2 MOI (multiplicity of infection). Cells were selected with 5 μg/mL blasticidin for at least 2 wk. The cells infected with empty virus vector were used as control cells in all experiments.

RNA Extraction and Real-Time PCR. RNA was extracted with Qiagen messenger RNA (mRNA) extraction kit according to manufacturer's protocol from cells grown in a six-well plate. cDNA was synthesized from 1 μg of total RNA with iScript first-strand cDNA synthesis kit according to manufacturer's protocol (Bio-Rad Laboratories, Inc.). Real-time PCR was performed with iTaq Universal SYBR Green supermix (Bio-Rad Laboratories, Inc.) on a 7500 Fast Real-Time PCR System (Applied Biosystems) using optimized conditions for SYBR Green I dye: 95 °C for 2 min, followed by 40 cycles at 95 °C for 15 s, 60 °C for 15 s, and 72 °C for 30 s. Optimum primer concentration was determined in preliminary experiments, and amplification specificity was confirmed by melt curve analysis. Relative gene expression was calculated using ΔΔCt using GAPDH as normalization control. Primer sequences for the real-time PCR were:

GAPDH; F, 5′-TGACAACTTTGGTATCGTGGAAGG-3′, and

R, 5′-AGGCAGGGATGATGTTCTGGAGAG-3′;

ERβ1, F, 5′-GTCAGGCATGCGAGTAACAA-3′ and

R, 5′-GGGAGCCCTCTTTGCTTTTA-3′;

INPP4B, F, AGAGCTTTAGATTGCATGAGAAGAGA, and

R, 5′-CCTCCTGCATTTGATATTCTTCAGT-3′.

All primers were designed using National Center for Biotechnology Information primer-BLAST and ordered from IDT.

RNA-seq and Transcriptomic Analysis. Libraries for RNA-seq were prepared with KAPA stranded RNA-seq kit. The workflow consisted of mRNA enrichment, cDNA generation, and end repair to generate blunt ends, A-tailing, adaptor ligation, and PCR amplification. Sequencing was performed on

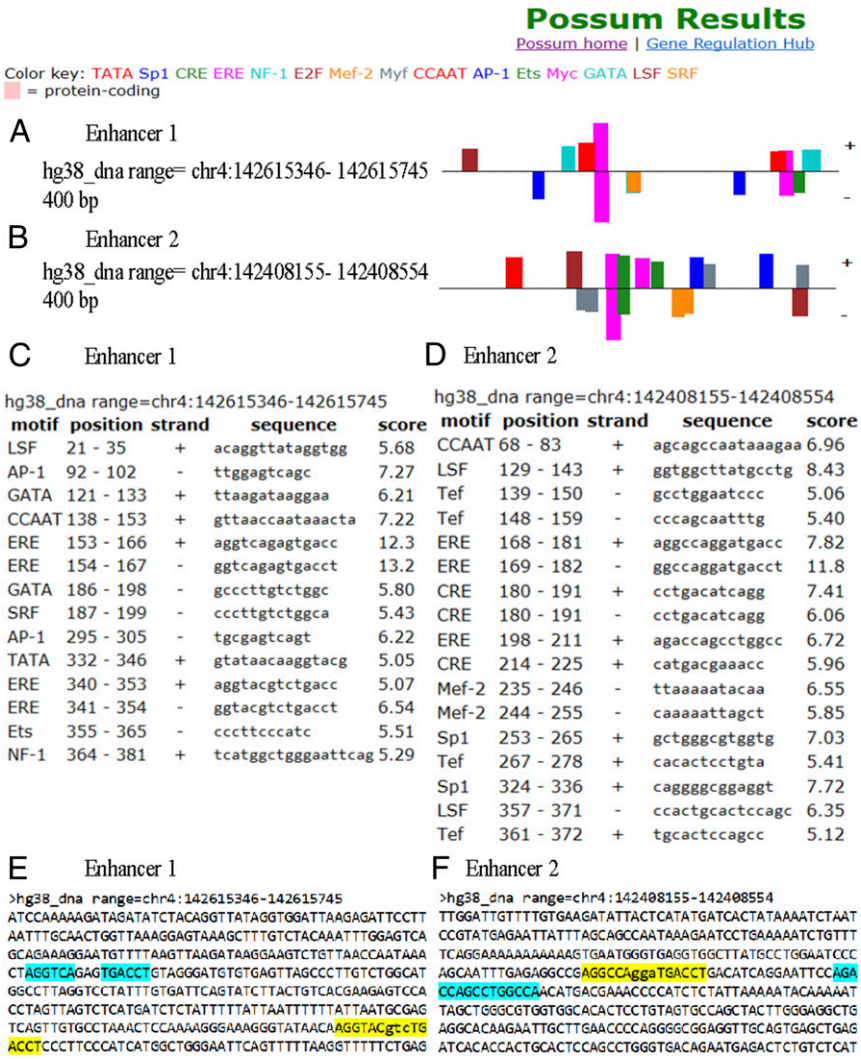

Fig. 8. Analysis of motifs enriched in ERβ1 binding regions in INPP4B. A DNA stretch of 400 bp centered around enhancer 1 and enhancer 2 was extracted and analyzed for cis-elements enrichment using Possum software. (*A* and *B*) Positioning of motifs in the enhancer 1 (*A*) and enhancer 2 (*B*). (*C* and *D*) List of motifs found in enhancer 1 (*C*) and enhancer 2 (*D*). (*E* and *F*) Sequences of enhancer 1 (*E*) and enhancer 2 (*F*), EREs are highlighted in green and yellow color.

Illumina HiSeq 3000 for a single read of 50 bp. The reads were mapped to the latest UCSC transcript set using Bowtie2 version 2.1.0 (42), and the gene expression level was estimated using RSEM v1.2.15 (43). TMM (trimmed mean of M-values) was used to normalize the gene expression across samples. Differentially expressed genes were identified using edgeR program (44). Genes showing altered expression with $P < 0.05$ and more than 1.5-fold changes were considered differentially expressed.

Protein Extract Preparation. To prepare whole-cell extracts, cells were washed twice with cold phosphate-buffered saline (PBS), scraped with a rubber policeman in PBS, and cell pellet was collected by centrifugation at 3,000 × *g* for 5 min. Cells were suspended in 10 times packed cell volume of RIPA lysis buffer (10 mM Tris·HCl pH 8.0, 1 mM ethylene diamino tetraacetic acid (EDTA), 0.5 mM ethylene glycol tetraacetic acid, 1% Triton X-100, 0.1% Sodium deoxycholate, 0.1% SDS, and 140 mM NaCl) supplemented with protease inhibitor mixture, and PhosStop (Roche), syringed 10 times through narrow needle and then centrifuged at 14,000 × *g* for 10 min. The clear supernatant was transferred to a new centrifuge tube, and protein concentration was measured using Pierce 660-nm protein assay kit (Thermo Fisher Scientific). Samples were prepared by boiling with 4× loading dye and β-mercaptoethanol.

Western Blotting. Thirty-five micrograms of protein were loaded on an SDS/PAGE 4–20% Bis-Tris gel with Tris running buffer and transferred to a polyvinylidene fluoride membrane after electrophoretic separation. Membranes were blocked with 5% nonfat powdered milk in 0.1% Tris-buffered saline buffer and probed with anti-ERβ (PPZ0506, Invitrogen), anti-INPP4B (D9K1B), pAKT Thr308 (D25E6), pAKT Ser473 (D9E), panAKT (C67E7), pGSK3β (D85E12), (Cell Signaling Technology), GAPDH-HRP (sc-47724) (Santa Cruz Biotechnology), and β-Actin (A19780) (Millipore Sigma). Primary antibodies were used at 1:200–1,000 dilutions, and secondary antibody was used at 1:10,000. The Western blot experiments were repeated at least three times.

Immunohistochemistry. Paraffin-embedded PCa array sections were deparaffinized in xylene, rehydrated through graded alcohol, and processed for antigen retrieval in 10 mM citrate buffer (pH 6.0) at 97 °C for 12 min in PT module. To quench endogenous peroxidase, sections were incubated in 0.6% H_2O_2 in 50% methanol for 20 min at room temperature. After washing with PBS for three times, sections were incubated in 3% bovine serum albumin for 30 min and a biotin blocking system (Dako) was used to block endogenous biotin. Sections were then incubated with anti-ERβ (1:100; made in our laboratory) or Anti-INPP4B (1:50; ab81269, Abcam) at 4 °C for overnight. After washing, sections were incubated with anti-chicken secondary antibody (1:200; Invitrogen) and anti-rabbit secondary antibody (1:200; Invitrogen) for 1 h at room temperature. After washing with PBS for three times, sections were incubated with the avidin–biotin complex (PK-6100, Vector Laboratories) for 1 h at room temperature followed by DAB (3,3′-Diaminobenzidine) as the chromogen. Sections were later counterstained with hematoxylin to label nuclei.

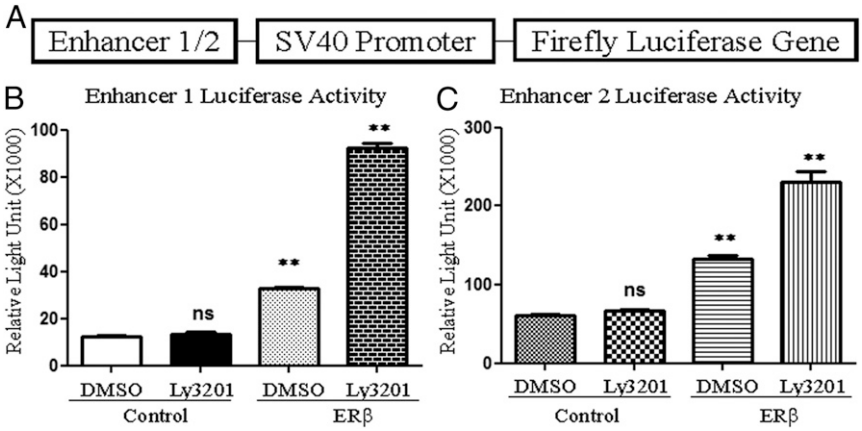

Fig. 9. ERβ1 transcriptional activity from INPP4B enhancers. PCR amplified product of enhancer 1 and enhancer 2 was cloned into pGL3 promoter luciferase vector and transfected into PC3 cells with or without ERβ1 expression plasmid. Luciferase activity was measured after treatment with DMSO or LY3201 for 18 h. (*A*) Schematic of the reporter construct. ERβ1 activity from enhancer 1 (*B*) and from enhancer 2 (*C*). ns, not significant.

ChIP. ChIP assay was modified from a previous report (45). Subconfluent PC3 cells (90%) were grown in a 100-mm dish and treated with indicated ligand for 24 h in 10% charcoal stripped serum. Cells were fixed with 1.5% formaldehyde by adding directly into the media into the plates for 10 min at room temperature, quenched with 0.125 M glycine, washed two times with cold PBS, scraped in PBS, and cells were collected by centrifugation. Cell pellets were suspended in 500 μl ChIP buffer (Tris·HCl 20 mM, NaCl 150 mM, EDTA 2 mM, Triton X-100 1%, SDS 0.1%, and protease inhibitor), sonicated with Diagenode UCD200 in ice-cold water for 60 cycles (30 s on/30 s off), and lysates were cleared by centrifugation at 14,000 rpm for 5 min. Following sonication, 25-μL samples were mixed with 75 μL of elution buffer (Tris·HCl 50 mM, EDTA 10 mM, 1% SDS), incubated at 65 °C for >6 h, and purified using PCR purification kit (Qiagen) for input DNA. The rest of the lysate was divided equally into two Eppendorf tubes, 10 μL of ERβ-LBD antibody (homemade) or 10 μL of hyperimmune rabbit IgG (Santa Cruz) was added and incubated at 4 °C O/N on slow rotation. On the next day, 20 μL of protein G beads (Dynabeads, Invitrogen) were added to IP samples and rotated at room temperature for 2 h. Beads were washed twice with 1 mL each of wash buffer II (Hepes 50 mM, NaCl 500 mM, EDTA 1 mM, Sodium Deoxycholate 0.1%, Triton X-100 1%), III (Tris·HCl 10 mM, LiCl 250 mM, EDTA 1 mM, sodium deoxycholate 0.5%, Nonidet P-40 0.5%), and IV (Tris·HCl 10 mM, EDTA 1 mM) for 2 min on a slow rotation at room temperature, then suspended in 100 μL of elution buffer and incubated at 65 °C for >6 h, and finally purified using PCR purification kit (Qiagen). Purified DNA was used for qPCR and sequencing. Fold enrichment was calculated using ΔΔCt method.

ChIP-seq Analysis. ChIP DNA samples were analyzed for quality and integrity on a Qbit 2.0 fluorometer (Thermo Fisher Scientific). Nextera DNA Flex Library prep kit was used for library preparation as per manufacturer's recommendation, and DNA was sequenced on an Illumina NextSeq 500. The reads were mapped to the latest UCSC genome build using Bowtie2 version 2.1.0. From the aligned reads, peaks were called and annotated using MACS2 (46). This methodology drew pairwise comparisons between each ChIP sample and control.

siRNA Transfection. siRNA for human INPP4B (catalog no. 4392420) and negative control (catalog no. 4390843) were purchased from Thermo Fisher Scientific. PC3-ERβ1 cells were grown to 50% confluency in complete medium and transfected with siRNA using Lipofectamine 2000 (Thermo Fisher Scientific) at the final concentration of 50 nM of each (control or INPP4B). After 48 h, cells were treated with DMSO (vehicle control) or 1 μM LY3201 in 10% DCC-FBS for 24 h, and RNA and protein was extracted. For scratch assay, subconfluent (70–80%) cells were transfected as above and, after 48 h, wound healing assay was performed.

Wound Healing Assay. PC3 cells expressing either ERβ1 or empty vector (control cells) were grown to confluency in a 12-well plate in Complete medium, then wounded with a 200-μL pipette tip, washed with PBS, 10% DCC was added with indicated treatment, and image was taken with an Olympus inverted microscope with Axiocam software. Cells were incubated at 37 °C with 5% CO_2 and 100% humidity for 18 h or 24 h. Images were taken again after the end of incubation. For wound healing assay comparing between control cells and ERβ1 cells, incubation was for 18 h, and for wound healing assay after siRNA transfection, incubation was for 24 h.

Luciferase Assay. A 500-bp sequence surrounding each of the ERβ1 binding enhancer sequences identified from ChIP-seq were amplified using PCR and cloned into pGL3 luciferase reporter in front of a minimal promoter. PC3 cells were grown to 50% confluency in a six-well plate and transfected with 1 μg of the luciferase constructs along with or without 0.5 μg of ERβ1 expression vector in 10% DCC medium. Twenty-four hours posttransfection, cells were treated with DMSO (vehicle control) or 10 nM LY3201 in fresh 10% DCC for 24 h more. The next day, media was aspirated, 200 μL of lysis buffer was added to cells in each well, and collected lysates were centrifuged at 14,000 × *g* for 10 min. Fifty microliters of cleared lysate was used to measure luminescence on a Perkin-Elmer Victor x luminescence plate reader using the luciferase kit from BioVision.

Statistical Analysis. Statistical analysis was performed with GraphPad Prism 8 software. Student's *t* test and one-way ANOVA were used for statistical analysis. Results were considered significant with P value < 0.05.

Data Availability. All study data are included in the article and supporting information.

ACKNOWLEDGMENTS. This study was supported by grants from the Brockman Foundation, the Robert A. Welch Foundation, and the Swedish Cancer Fund.

1. R. L. Siegel, K. D. Miller, A. Jemal, Cancer statistics, 2019. *CA Cancer J. Clin.* **69**, 7–34 (2019).
2. M. S. Litwin, H. J. Tan, The diagnosis and treatment of prostate cancer: A review. *JAMA* **317**, 2532–2542 (2017).
3. M. Shariati, F. Meric-Bernstam, Targeting AKT for cancer therapy. *Expert Opin. Investig. Drugs* **28**, 977–988 (2019).
4. G. Song, G. Ouyang, S. Bao, The activation of Akt/PKB signaling pathway and cell survival. *J. Cell Mol. Med.* **9**, 59–71 (2005).
5. T. Maehama, J. E. Dixon, The tumor suppressor, PTEN/MMAC1, dephosphorylates the lipid second messenger, phosphatidylinositol 3,4,5-trisphosphate. *J. Biol. Chem.* **273**, 13375–13378 (1998).
6. T. Jamaspishvili *et al.*, Clinical implications of PTEN loss in prostate cancer. *Nat. Rev. Urol.* **15**, 222–234 (2018).
7. H. M. Wise, M. A. Hermida, N. R. Leslie, Prostate cancer, PI3K, PTEN and prognosis. *Clin. Sci. (Lond.)* **131**, 197–210 (2017).
8. B. S. Taylor *et al.*, Integrative genomic profiling of human prostate cancer. *Cancer Cell.* **18**, 11–22 (2010).
9. C. Gewinner *et al.*, Evidence that inositol polyphosphate 4-phosphatase type II is a tumor suppressor that inhibits PI3K signaling. *Cancer Cell.* **16**, 115–125 (2009).
10. C. Li Chew *et al.*, In vivo role of INPP4B in tumor and metastasis suppression through regulation of PI3K-AKT signaling at endosomes. *Cancer Discov.* **5**, 740–751 (2015).
11. S. Kofuji *et al.*, INPP4B is a PtdIns(3,4,5)P3 phosphatase that can act as a tumor suppressor. *Cancer Discov.* **5**, 730–739 (2015).

12. N. K. Rynkiewicz *et al*., INPP4B is highly expressed in prostate intermediate cells and its loss of expression in prostate carcinoma predicts for recurrence and poor long term survival. *Prostate* **75**, 92–102 (2015).
13. J. Hartman *et al*., Tumor repressive functions of estrogen receptor beta in SW480 colon cancer cells. *Cancer Res.* **69**, 6100–6106 (2009).
14. G. R. Sareddy *et al*., Selective estrogen receptor beta agonist LY500307 as a novel therapeutic agent for glioblastoma. *Sci. Rep.* **6**, 24185 (2016).
15. A. Strom *et al*., Estrogen receptor beta inhibits 17beta-estradiol-stimulated proliferation of the breast cancer cell line T47D. *Proc. Natl. Acad. Sci. U.S.A.* **101**, 1566–1571 (2004).
16. W. F. Wu *et al*., Estrogen receptor beta, a regulator of androgen receptor signaling in the mouse ventral prostate. *Proc. Natl. Acad. Sci. U.S.A.* **114**, E3816–E3822 (2017).
17. P. Dey *et al*., Estrogen receptors beta1 and beta2 have opposing roles in regulating proliferation and bone metastasis genes in the prostate cancer cell line PC3. *Mol Endocrinol.* **26**, 1991–2003 (2012).
18. P. Dey, A. Ström, J. A. Gustafsson, Estrogen receptor β upregulates FOXO3a and causes induction of apoptosis through PUMA in prostate cancer. *Oncogene* **33**, 4213–4225 (2014).
19. C. Thomas *et al*., ERbeta1 represses basal breast cancer epithelial to mesenchymal transition by destabilizing EGFR. *Breast Cancer Res.* **14**, R148 (2012).
20. I. Bado, F. Nikolos, G. Rajapaksa, J. A. Gustafsson, C. Thomas, ERbeta decreases the invasiveness of triple-negative breast cancer cells by regulating mutant p53 oncogenic function. *Oncotarget* **7**, 13599–13611 (2016).
21. A. F. Levakov *et al*., The expression and localization of estrogen receptor beta in hyperplastic and neoplastic prostate lesions. *Vojnosanit. Pregl.* **72**, 906–913 (2015).
22. I. Leav *et al*., Comparative studies of the estrogen receptors beta and alpha and the androgen receptor in normal human prostate glands, dysplasia, and in primary and metastatic carcinoma. *Am. J. Pathol.* **159**, 79–92 (2001).
23. T. Fixemer, K. Remberger, H. Bonkhoff, Differential expression of the estrogen receptor beta (ERbeta) in human prostate tissue, premalignant changes, and in primary, metastatic, and recurrent prostatic adenocarcinoma. *Prostate* **54**, 79–87 (2003).
24. J. S. Lai *et al*., Metastases of prostate cancer express estrogen receptor-beta. *Urology* **64**, 814–820 (2004).
25. K. Lindberg, L. A. Helguero, Y. Omoto, J. Å. Gustafsson, L. A. Haldosén, Estrogen receptor β represses Akt signaling in breast cancer cells via downregulation of HER2/HER3 and upregulation of PTEN: Implications for tamoxifen sensitivity. *Breast Cancer Res.* **13**, R43 (2011).
26. K. M. Lau, M. LaSpina, J. Long, S. M. Ho, Expression of estrogen receptor (ER)-alpha and ER-beta in normal and malignant prostatic epithelial cells: Regulation by methylation and involvement in growth regulation. *Cancer Res.* **60**, 3175–3182 (2000).
27. M. E. Kaighn, K. S. Narayan, Y. Ohnuki, J. F. Lechner, L. W. Jones, Establishment and characterization of a human prostatic carcinoma cell line (PC-3). *Invest. Urol.* **17**, 16–23 (1979).
28. S. Tai *et al*., PC3 is a cell line characteristic of prostatic small cell carcinoma. *Prostate.* **71**, 1668–1679 (2011).
29. S. W. Hayward *et al*., Establishment and characterization of an immortalized but non-transformed human prostate epithelial cell line: BPH-1. *In Vitro Cell. Dev. Biol. Anim.* **31**, 14–24 (1995).
30. V. S. Bansal, K. K. Caldwell, P. W. Majerus, The isolation and characterization of inositol polyphosphate 4-phosphatase. *J. Biol. Chem.* **265**, 1806–1811 (1990).
31. K. P. Hoeflich *et al*., Requirement for glycogen synthase kinase-3beta in cell survival and NF-kappaB activation. *Nature* **406**, 86–90 (2000).
32. L. G. Rodriguez, X. Wu, J. L. Guan, Wound-healing assay. *Methods Mol. Biol.* **294**, 23–29 (2005).
33. A. Grada, M. Otero-Vinas, F. Prieto-Castrillo, Z. Obagi, V. Falanga, Research techniques made simple: Analysis of collective cell migration using the wound healing assay. *J. Invest. Dermatol.* **137**, e11–e16 (2017).
34. W. Xu, Z. Yang, N. Lu, A new role for the PI3K/AKT signaling pathway in the epithelial-mesenchymal transition. *Cell Adh. Migr.* **9**, 317–324 (2015).
35. J. Wang *et al*., POSSUM: A bioinformatics toolkit for generating numerical sequence feature descriptors based on PSSM profiles. *Bioinformatics* **33**, 2756–2758 (2017).
36. M. Jia, K. Dahlman-Wright, J. A. Gustafsson, Estrogen receptor alpha and beta in health and disease. *Best Pract. Res. Clin. Endocrinol. Metab.* **29**, 557–568 (2015).
37. M. C. Hodgson *et al*., INPP4B suppresses prostate cancer cell invasion. *Cell Commun. Signal.* **12**, 61 (2014).
38. H. Chen, H. Li, Q. Chen, INPP4B overexpression suppresses migration, invasion and angiogenesis of human prostate cancer cells. *Clin. Exp. Pharmacol. Physiol.* **44**, 700–708 (2017).
39. D. D. Sarbassov, D. A. Guertin, S. M. Ali, D. M. Sabatini, Phosphorylation and regulation of Akt/PKB by the rictor-mTOR complex. *Science* **307**, 1098–1101 (2005).
40. M. C. Hodgson *et al*., Decreased expression and androgen regulation of the tumor suppressor gene INPP4B in prostate cancer. *Cancer Res.* **71**, 572–582 (2011).
41. L. Sun *et al*., Ipatasertib, a novel Akt inhibitor, induces transcription factor FoxO3a and NF-κB directly regulates PUMA-dependent apoptosis. *Cell Death Dis.* **9**, 911 (2018).
42. B. Langmead, S. L. Salzberg, Fast gapped-read alignment with Bowtie 2. *Nat Methods.* **9**, 357–359 (2012).
43. B. Li, C. N. Dewey, RSEM: accurate transcript quantification from RNA-Seq data with or without a reference genome. *BMC Bioinformatics.* **12**, 323 (2011).
44. M. D. Robinson, D. J. McCarthy, G. K. Smyth, edgeR: A bioconductor package for differential expression analysis of digital gene expression data. *Bioinformatics* **26**, 139–140 (2010).
45. H. Mohammed *et al*., Rapid immunoprecipitation mass spectrometry of endogenous proteins (RIME) for analysis of chromatin complexes. *Nat. Protoc.* **11**, 316–326 (2016).
46. Y. Zhang *et al*., Model-based analysis of ChIP-Seq (MACS). *Genome Biol.* **9**, R137 (2008).